Dimensionality crossovers of the σ plasmon in coaxial carbon nanotubes

C. Yannouleas, E. N. Bogachek, and Uzi Landman
School of Physics, Georgia Institute of Technology, Atlanta, Georgia 30332-0430
(Received 5 May 1994)

Dimensionality crossovers of plasmons in carbon nanotubes, modeled as curved layered electron-gas superstructures, are investigated. For small wave vectors, the σ plasmons exhibit a transition from a one- to a three-dimensional character as the number of graphitic shells increases, in correspondence with recent experiments. For large wave vectors, plasmons of two-dimensional character are predicted.

Investigations of plasmon excitations in the recently discovered carbon nanotubes,[1] and the ability to prepare such structures with variable numbers of coaxial shells, offer unique opportunities for exploration of the effects of dimensionality on the nature of collective excitations in curved low-dimensional electron-gas superstructures. A similar issue was studied previously for planar geometry in the context of layered two-dimensional-electron-gas (2DEG) semiconductor systems, where an evolution[2] to bulk layered-electron-gas behavior[3,4] was found as a function of the number of planar layers.

Most recently electron energy loss spectroscopy (EELS) of carbon nanotubes[5–7] has revealed a volume plasmon at energies around 24 eV–27 eV for carbon nanotubes comprising at least 25–30 coaxial graphitic shells, and a shift to lower energies, as low as 15 eV,[5] for nanotubes with a small number of shells. While several theoretical studies of plasmon excitations in carbon nanotubes have appeared,[8–10] the evolution and character of the plasmon as a function of the number of shells were not addressed.

In this paper, we show that an assembly of coaxial carbon nanotubules constitutes a unique superlattice-type arrangement, where a succession of dimensionality crossovers (from one to three, and then to two dimensions) can occur as a function of the number of graphitic sheets and of the σ-plasmon wavelength, $\lambda = 2\pi/q$, q being the wave vector of the plasmon. Such crossovers may account for the main experimentally observed trends.[5,6]

The σ electrons of each graphitic cylindrical sheet can be viewed as an electron gas confined on the surface of a cylinder of radius R. As a result, the corresponding plasmon excitations in most instances have a one-dimensional character, namely, the plasmon energies are given[10,11] by

$$\omega_0(q \approx 0) = \omega_R R q [2\ln(1.123/Rq)]^{1/2}\ ,\ m = 0 \qquad (1)$$

$$\omega_m(q = 0) = \omega_R \sqrt{m}\ ,\ m \geq 1, \qquad (2)$$

where $m \geq 0$ denotes the plasmon modes corresponding to the projection of the angular momemtum, and

$$\omega_R = [4\pi e^2 (n/2R)/m_e]^{1/2}\ , \qquad (3)$$

with n being the areal electronic density on the tubule and m_e the electron mass. We note that for $m = 0$ the plasmon dispersion varies linearly with q (with an additional weak logarithmic dependence), while for $m \neq 0$ the plasmon energies for $q = 0$ are finite and depend on $1/\sqrt{R}$, reflecting the energy gaps between the subbands. Equations (1) and (2) describe the behavior of a 1DEG, which is different from the $q^{1/2}$ dependence of the 2DEG, and the $\omega_p + cq^2$ behavior of the 3DEG (ω_p is the bulk plasmon frequency as $q \to 0$). Nevertheless, it has been shown that under certain conditions, namely, $qR \gg 1$ and $k_F R \gg 1$ [where $k_F = (2\pi n)^{1/2}$ is the Fermi wave vector], an isolated solid or hollow narrow tubule can exhibit[9,10,12,13] a two-dimensional electron gas behavior.

For an isolated cylindrical graphitic sheet with radius R (even for one with the smallest radius $6.4a_0$, where a_0=0.5292 Å is the Bohr radius), the areal density of the σ electrons is rather high (namely, $0.319a_0^{-2}$), and the condition $k_F R \approx 9.1 \gg 1$ is well satisfied. In this limit, the index m can be treated as a continuous variable and the free polarizability D^0 of the σ electrons can be calculated in a closed form,[10]

$$D^0 = \mathbf{Q}^2 R k_F^2/(2\pi m_e \omega^2) = \mathbf{Q}^2 R n/(m_e \omega^2)\ , \qquad (4)$$

where $\mathbf{Q}$ is a two-dimensional wave vector equal to $(m/R, q)$, q being the collective wave vector parallel to the symmetry axis.

Apart from a factor R, expression (4) agrees with the free polarizability of a 2DEG (see Ref. 2). The frequencies of collective modes of the tubule are those for which the dielectric function vanishes, i.e., they are solutions of the equation

$$1 - V(\mathbf{Q}) D^0 = 0\ . \qquad (5)$$

In Eq. (5), $V(\mathbf{Q})$ is the Fourier transform of the Coulomb force in cylindrical coordinates, given by[14]

$$V(\mathbf{Q}, r_i, r_j) = 4\pi e^2 I_m(q r_<) K_m(q r_>)\ , \qquad (6)$$

where I_m and K_m are the modified Bessel functions, and $r_> = \max(r_i, r_j)$ and $r_< = \min(r_i, r_j)$ (on the same tubule $r_i = r_j = R$). For the tubule to be a 2DEG, V must exhibit the behavior of the two-dimensional Fourier transform of the Coulomb force, namely, $2\pi e^2/q$. In the case of a single tubule, expression (6) reduces to this limit

when $qR \gg 1$, as can be seen by using the well known asymptotic expansions[14]

$$I_m(x) \to \frac{1}{\sqrt{2\pi x}} e^x;\ K_m(y) \to \sqrt{\frac{\pi}{2y}} e^{-y};\ x, y \gg 1. \quad (7)$$

For values $q \gg m/R$, the plasmon dispersion is indeed proportional to $q^{1/2}$ independently of the value of m.

For two or more coupled coaxial tubules (shells), we can generalize Eq. (5) by following the self-consistent-field (also known as RPA) method,[15] leading to a matrix equation[4]

$$U_i = \sum_{j=1}^{N} M_{ij} U_j \ , \quad (8a)$$

where the indices (i, j) correspond to different tubules, whose total number is N. The vector $\mathbf{U}$ denotes the amplitude of the induced field, $u_j(q, \omega) = U_j \exp(-iqz - i\omega t)$ on each tubule, and the nonsymmetric matrix $\mathbf{M}$ has elements

$$M_{ij} \equiv V(\mathbf{Q}, R_i, R_j) D_j^0 \quad (8b)$$
$$= \frac{4\pi e^2 n}{m_e \omega^2} R_j \left[\left(\frac{m}{R_j} \right)^2 + q^2 \right] I_m(qR_<) K_m(qR_>) \ .$$

Qualitative insight can be gained by considering certain limiting situations. Indeed, considering plasmons with wavelengths much smaller than the innermost radius R_1, so that $qR_1 \gg 1$, we can apply the asymptotic expansion (7) to all tubule indices i and j. Additionally, assuming that the width Δ of the hollow cylindrical superlattice is small compared to the innermost tubule radius (i.e., $\Delta/R_1 \ll 1$), we can treat the magnitudes of all tubule radii as equal in the exponential prefactors [see Eq. (7)], and consider only effects due to the length differences, $R_< - R_> = -|R_i - R_j|$, in the exponents. With the further approximation that sufficiently many shells can be packed within the inner and outer radii (i.e., $d/\Delta \ll 1$, d is the intertubule distance), the limits over the j summation in Eq. (8a) can be extended from $-\infty$ to $+\infty$. Then Eq. (8a) simplifies to the following dispersion relation (when $q \gg m/R_1$)

$$1 = [2\pi e^2 nq/(m_e \omega^2)] S(q) \ , \quad (9)$$

where $S(q)$ is given by

$$S(q) = \sum_j e^{-q|R_i - R_j|} = \sum_j e^{-q|i-j|d} \ . \quad (10)$$

Furthermore in this case, the summation over j yields $S(q) = \coth(qd/2)$.

In the weak coupling limit, $qd \gg 1$, the tubules decouple, each shell responds independently with its own two-dimensional plasmon, and the collective excitation of the assembly is

$$\omega \approx (2\pi e^2 n/m_e)^{1/2} q^{1/2} \ . \quad (11)$$

In the opposite strong coupling limit, $qd \ll 1$, $\coth(qd/2) \approx 2/qd$, and the super-structure has a plasmon with energy

$$\omega_p \approx [4\pi e^2 n/(m_e d)]^{1/2} \ . \quad (12)$$

The ratio n/d defines an effective volume density, and Eq. (12) represents the corresponding volume (3D) plasmon.

We note that Eqs. (11) and (12) recover the results of Fetter,[3] obtained for a planar geometry, since the wavelength of the plasmon, λ, was taken by us to be small compared to the inner radius R_1 (i.e., $qR_1 \gg 1$). The finite value of the curvature reasserts itself as soon as $qR_N \ll 1$, when the assembly reverts to a 1DEG behavior (see discussion below in connection with Fig. 3).

While the analytic results demonstrating the emergence of the volume plasmon in coaxial tubules (as well as the crossover from 1DEG to 3DEG) were obtained above for certain idealized circumstances (e.g., $d \ll \Delta \ll R_1$), our numerical study of the solutions of Eq. (8) shows that similar behavior maintains also for cases corresponding to actual carbon nanotubes (i.e., when $R_1 = d = 6.4a_0$).

Figure 1 displays the solutions of Eq. (8) as a function of the number N of carbon tubules when the wave vector $q = 0.02a_0^{-1}$. For this value of q, one has $qR_1 = qd = 0.128$ (strong coupling), and as a result the response of tubules with only a few shells approximates the response of a 1DEG. Indeed, from Fig. 1(a), the value for $N = 1$ and $m = 1$ is $\hbar\omega_1 = 15.19$ eV, in agreement with expression (2) for $q = 0$. However, as the radius $R_N = Nd$ of the outermost tubule increases, the product qR_N becomes larger than unity, which as aforementioned would lead to a 2DEG behavior for individual tubules and to the development of a 3D plasmon due to the intertubule couplings. The onset of such a crossover from a 1D to a 3D behavior is expected when N reaches a value such

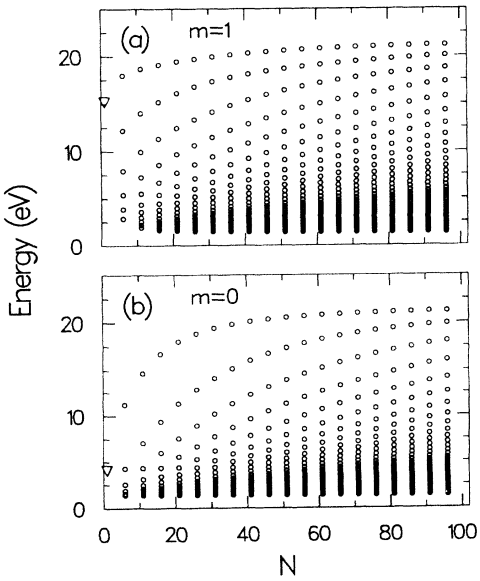

FIG. 1. Solutions for $q = 0.02a_0^{-1}$ versus the number of shells, N, in the carbon nanotube. The innermost radius $R_1 = d$, where $d = 6.4a_0$ is the intertubule distance. Solutions for $N = 1$ are denoted by a triangle. (a) The $m = 1$ mode. (b) The $m = 0$ mode.

that $qR_N \approx 1$, or $N \approx 8$ for $q = 0.02a_0^{-1}$. For $N \geq 30$, the N solutions of Eq. (8) form a band, bounded between upper and lower limits, independent of N. As discussed in the case of finite planar superlattices[2] such behavior is characteristic of a 3DEG. The top of the band is the 3D plasmon and carries most of the oscillator strength. Indeed, taking the areal density of the σ electrons to be $n = 0.319a_0^{-2}$, and applying expression (12), the value of the bulk plasmon is 21.53 eV (using the bare electron mass[16]), which practically coincides[17] with the value at the top of the band [see Fig. 1(a)].

For $m = 0$ [Fig. 1(b)], the one-dimensional behavior described by Eq. (1) is reproduced. Indeed, for $N = 1$, the plasmon has a value close to zero, unlike the finite value of the $m = 1$ case. In spite of the different behavior for the first few tubules, both modes develop the same volume band for $N \geq 30$. In particular, the top and bottom limits in both bands are similar in value.

In Fig. 2(a), we exhibit the development of the 3D plasmon for $N = 30$, as a function of the wave vector q. Note that for $q \leq 0.04a_0^{-1}$, the superlattice behaves as a 1DEG, while in the region $0.05 \leq q \leq 0.10$ a 3DEG develops, since the top of the band is very close to the 3D plasmon, i.e., 21.53 eV (see inset). For values $q \geq 0.3a_0^{-1}$, the coaxial tubules decouple from each other, and the superstructure exhibits a $q^{1/2}$ behavior characteristic of a 2DEG. Figure 2(b) displays the behavior of an assembly for $N = 5$ tubules as a function of q. It is apparent that the top of the five-level band does not saturate near the value of 21.53 eV, and consequently the dominant collective mode for an assembly of a small number of tubules passses from the 1DEG case directly to the 2DEG behavior without an intermediate 3D behavior (this result is in agreement with that of Ref. 10, where the case $N \leq 4$ was studied).

Finally, Fig. 3(a) displays the behavior of a coaxial-tubules superstructure as a function of N when $q = 0$. In this case, $qR_N = 0$ for all radii, and one expects a 1DEG behavior. As an example, we have considered the case with an innermost radius $R_1 = 5d$. As Fig. 3(a) shows, increasing the number N of tubules produces a band that has certain similarities with the 3D band of Fig. 1(a). However, the top of the band saturates at values which depend on the inner radius and are different from the value 21.53 eV of the 3D plasmon. To demonstrate this point, we show in Fig. 3(b) the top of the $m = 1$ bands for the case of an assembly of $N = 100$ tubules as a function of q for different values of the innermost radius ($R_1 = 1d$, $5d$, $10d$, $20d$, $40d$). Near $q = 0$, the top of the band depends strongly on the value of the inner radius (1DEG behavior). However, when q increases one observes a crossover to a 3DEG behavior, since all the curves converge rapidly to the 3D-plasmon value (21.53 eV).

In summary, we showed the following.

(I) For small q, such that $qR_1 = qd < 1$ (strong coupling), a transition from a characteristic 1D to a 3D bulk-plasmon behavior may occur upon increase of the number of shells (N) comprising the nanotube [(e.g., onset of such a transition is predicted to occur at $N \approx 10$ for $q = 0.02a_0^{-1}$, and may depend on q); see Fig. 1].

(II) For a multishell nanotube (large N), the character

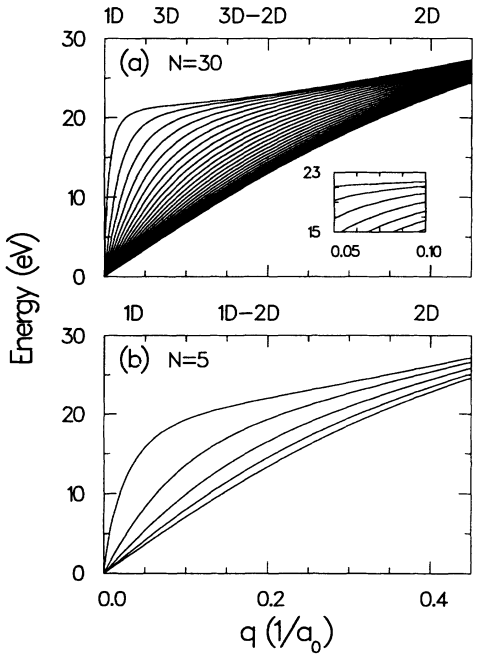

FIG. 2. Solutions for the $m = 0$ mode for a carbon nanotube with a fixed number of shells, N, vs the wave vector q. The innermost radius $R_1 = d$, where $d = 6.4a_0$ is the intertubule distance. The dimensionalities of the plasmons are indicated at the top. (a) $N = 30$ shells. (b) $N = 5$ shells.

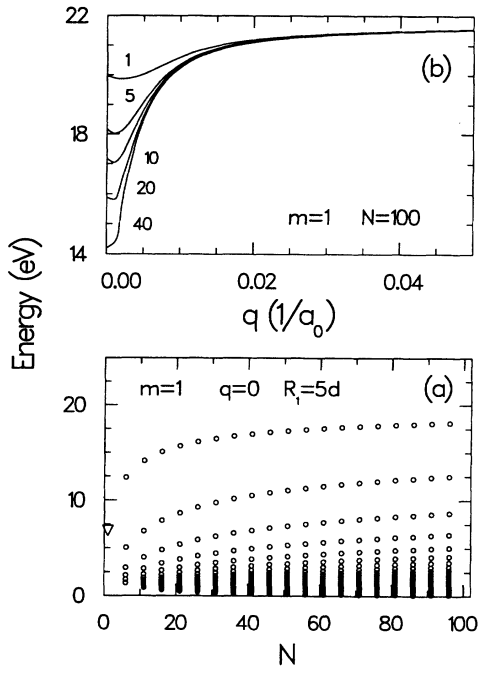

FIG. 3. (a) Solutions for the $m = 1$ mode for $q = 0$, vs the number of shells, N, in the carbon nanotube. The innermost radius $R_1 = 5d$, where $d = 6.4a_0$ is the intertubule distance. (b) The top level of the $m = 1$ band for several carbon nanotubes with $N = 100$ shells, versus q. Numbers label nanotubes with innermost radii $R_1 = d, 5d, 10d, 20d, 40d$.

of the collective σ excitation changes from a 1D plasmon for small values of q to a 2D plasmon for large q (decoupling regime of the excitations of individual layers), with the occurence of an intermittent 3D plasmon for a certain range of intermediate values of q; see Fig. 2.

(III) The nature of the crossover from 1D to 3D behavior of the plasmons for small q depends strongly on the value of the innermost radius of the nanotube; see Fig. 3.

Most pertinent to our discussion are the observation[6] of a systematic downward shift in the plasmon energy as the size of the nanotube (number of layers, N) is reduced, and the detection[5] of a 15 eV plasmon for nanotubes with $N < 12$ as well as the development of a graphiticlike bulk plasmon at 24 eV [or 27 eV (Ref. 6)], for larger N. These observations were interpreted by either invoking an effect of the π electrons on the σ-electrons collective excitation,[6] or by conjecturing[5] that the 15 eV plasmon corresponds to a surface plasmon (i.e., $\omega_s = \omega_p/\sqrt{2}$), in conjunction with conformal invariance.[5]

A fully quantitative comparison of theory with these measurements requires knowledge of the momentum transfer q (which was not reported in these experiments) as well as possible improvements of our theoretical model (e.g., including coupling between the σ and π electrons and/or considering the finite width of each individual carbon tubule). Nevertheless, the main trends found in these measurements may be explained in the framework of our model. Accordingly, we suggest that in such experiments for small q ($qd \ll 1$), the plasmons in nanotubes with a small number of shells (i.e., as long as the outermost radius R_N is smaller than $1/q$) are of 1D character, shifting to 3D plasmons as the number of shells increases (Fig. 1). We believe that this is the case pertaining to the current experiments.[5–7] Furthermore the 1D plasmons, and thus the nature of the transition to the 3D plasmon, is predicted to depend on the radius R_1 of the innermost tubule (Fig. 3). On the other hand, for $qd \gg 1$, we predict 2D plasmon characteristics for all number of shells N and all values of R_1, since $R_1 \geq d$ (Fig. 2). For a range of intermediate values of q ($qd \approx 1$) mixed character situations may arise. For example, in the case $R_1 = d$, a transition from an intermediate 1D-2D behavior for small N to an intermediate 3D-2D behavior occurs as the number of shells N increases (Fig. 2). Finally, our results suggest that systematic investigations of the nature of dimensionality crossovers of the plasmon in carbon nanotubes would require experimental energy-loss data as a function of the momentum transfer.

This research is supported by the U.S. Department of Energy, Grant No. FG05-86ER45234.

[1] S. Iijima, Nature **354**, 56 (1991).
[2] J.K. Jain and Ph.B. Allen, Phys. Rev. Lett. **54**, 2437 (1985).
[3] A.L. Fetter, Ann. Phys. (N.Y.) **81**, 367 (1973); **88**, 1 (1974).
[4] S. Das Sarma and J.J. Quinn, Phys. Rev. B **25**, 7603 (1982).
[5] L.A. Bursill, P.A. Stadelmann, J.L. Peng, and S. Prawer, Phys. Rev. B **49**, 2882 (1994).
[6] P.M. Ajayan, S. Iijima, and T. Ichihashi, Phys. Rev. B **47**, 6859 (1993).
[7] R. Kuzuo, M. Terauchi, and M. Tanaka, Jpn. J. Appl. Phys. **31**, L1484 (1992).
[8] M.F. Lin and W.-K. Shung, Phys. Rev. B **47**, 6617 (1993).
[9] O. Sato, Y. Tanaka, M. Kobayashi, and A. Hasegawa, Phys. Rev. B **48**, 1947 (1993).
[10] P. Longe and S.M. Bose, Phys. Rev. B **48**, 18 239 (1993).
[11] E.N. Bogachek and G.A. Gogadze, Zh. Eksp. Teor. Fiz. **67**, 621 (1974) [Sov. Phys. JETP **40**, 306 (1975)].
[12] H. Chen, Y. Zhu, and S. Zhou, Phys. Rev. B **36**, 8189 (1987).
[13] Y. Zhu, F.-Y. Huang, X.-M. Xiong, and S.-X. Zhou, Phys. Rev. B **37**, 8992 (1988).
[14] J.D. Jackson, *Classical Electrodynamics*, 2nd ed. (Wiley, New York, 1975), Sect. 3.11.
[15] H. Ehrenreich and M.H. Cohen, Phys. Rev. **115**, 786 (1959).
[16] The experimental values of the bulk plasmon in polycrystalline graphite, 27 eV, or 24 eV for oriented graphite (Ref. 5), reflect coupling between the σ and π electrons, while in our model only the σ electrons are considered.
[17] The contribution of cq^2 can be neglected, since $c = 12.93$ eV a_0^2 (see Ref. 4 for the expression relating c to k_F) so that one has $cq^2 = 0.0052$ eV for $q = 0.02a_0^{-1}$.